

Precipitation Kinetics in Age Hardening Al-alloys by Dilatometry and Differential Scanning Calorimetry

Manoj Kumar¹, Cecilia Poletti¹, Claire Collet² and H. Peter Degischer¹

¹Institute of Material Science and Technology TU Vienna, E308/13, Karlsplatz 1040, Austria

²University of Bordeaux 1, 351, cours de la Liberation, 33405 Talence, France

The precipitation and dissolution of precipitates during heat treatments in the age-hardenable aluminium alloys are very complex due to the influence of various parameters such as exact chemical composition and thermal history. The temperature dependence of the instantaneous thermal expansion coefficient was measured after different heat treatments by dilatometry and correlated with the heat evolution in differential scanning calorimetry. During continuous heating in the dilatometer, precipitation and dissolution of Zn₂Mg phases in an AW7020 alloy show retardation and acceleration in the expansion with respect to pure Al, respectively. Si precipitation results in an acceleration of the expansion in AW6016 alloy during heating, while Mg₂Si precipitation and dissolution do not affect the dilatometry curve, which behaves like pure Al. Superimposed endo- and exothermic peaks from thermograms can be correlated to the dilatometer curves of the alloys which indicate the phase changes caused by changes in the atomic volume, i.e. Si and Zn₂Mg precipitation. The dilatometry proved to be a complementary technique for differential scanning calorimetry to distinguish some steps within the precipitation kinetics.

Keywords: Al-Zn-Mg alloy, Al-Mg-Si alloy, Precipitation, DSC, Dilatometry.

1. Introduction

Demand for higher fuel efficiency and lesser pollution of transport systems is increasing, and this pushes industry to use more light alloys [1]. AW7xxx and AW6xxx are age hardenable Al wrought alloys with good corrosion resistance, high bending stiffness and strength to weight ratio which compete with steel for structural parts in cars [2]. Mg, Si, Zn and Cu are the most common alloying elements present in these Al alloys. High strength of Al-Zn-Mg based 7xxx alloys is the result of a fine dispersion of semi-coherent precipitates produced by artificial ageing after solution quenching. The precipitation sequence for Cu-free 7xxx Al-Zn-Mg alloys is usually proposed [3-6] to proceed as: α -supersaturated solid solution \rightarrow GPI Zones \rightarrow R \rightarrow dissolution of GPI/R $\rightarrow \eta'$ \rightarrow η -MgZn₂ or T-phase. The 6xxx Al-Mg-Si alloy is strengthened by precipitation of coherent and semi-coherent metastable phases containing Mg and Si atoms in different proportions depending on the composition of the alloy and the nucleation process. The precipitation sequence in excess-Si type Al-Mg-Si alloys is [7-8]: α -supersaturated solid solution \rightarrow Mg + Si clusters \rightarrow GP Zones \rightarrow dissolution of GP Zones $\rightarrow \beta''$ \rightarrow B' / β' + Si $\rightarrow \beta$ -Mg₂Si + Si.

The average atomic volume of Al is $16.50 \times 10^{-30} \text{ m}^3 \text{ atom}^{-1}$. The substitutional solute atoms differ slightly in their atomic radii changing the average atomic volume of the fcc-unit cell: Mg in solution increases the atomic volume by ca. 40%, while it decreases due to Zn [9] and Si by about 16% and 8 %, respectively. The negligible solubility of these elements tends to precipitate Si, Mg₂Si and MgZn₂. The precipitation of Si as a cubic diamond structure causes an increase of the average atomic volume by about 30% [10, 11]. The precipitation of Mg₂Si compensates the segregation of the solute resulting in a change of atomic volume <10%. The segregation of one Mg-atom and 2 Zn-atoms forming hcp structure MgZn₂ create a decrease in average atomic volume with respect to Al. 1/3 of any volume change can be measured by linear dilatometry (DIL). There are some dilatometric measurements made on Al-Mg-Si alloys to study the early stage precipitation effects

[12] and on Al-Si alloys to study the precipitation of Si [13-15]. Some results are also available on precipitation kinetic study of 7xxx aluminium alloys using DIL [16-17]. Differential scanning calorimetry (DSC) is a widely accepted tool to study the precipitation kinetics in alloys applying constant heating rates. This paper is an attempt to compare the results obtained from DIL and DSC of the AlZn4.5Mg1 alloy AW 7020 and of Si in the AlMgSi1 alloy AW6016 compared with the stoichiometric AW6061 alloy to conclude on the precipitation kinetics.

2. Experimental procedure

The studied alloys are AW7020: Al-4.58Zn-1.19Mg, AW6016: Al-0.55Mg₂Si-0.86Si and AW6061: Al-1.43Mg₂Si without Si surplus. AW7020 was delivered as tubes in T1 condition i.e. hot extruded at 480°C, air cooled and naturally aged. AW6016 and AW6061 alloy were delivered as rolled sheets in T4 condition (solution treated at 550°C, water quenched and naturally aged >1 year).

Solution quenched conditions are denominated T4f (fresh), if the measurements were performed immediately after quenching or when the quenched samples have been stored in liquid nitrogen before testing. The AW7020 samples were solution treated at 480°C for 20 min and water quenched. T4f samples were isothermally aged at temperatures between 150-250°C for periods from 1 to 24 h. AW7020 T4 (solution quenched and 4 days of natural ageing) and T6, i.e. T4 + 2 step ageing (90°C/8h + 145°C/15h) were also prepared. AW6016 alloy was solution heat treated at 550°C for 20 min and water quenched (T4f). A slowly cooled sample of AW6016 was prepared with a cooling rate of 1K/min from the solution treatment temperature to vary the nucleation condition (T4s). AW6016 T4f and T4 were continuously heated to 270°C (T4fa, T4a) and to 350°C (T4fb, T4b) with 10K/min and cooled with 50K/min to RT before repeating the DIL and DSC analysis up to 550°C.

Dilatometer tests were carried out in a TMA 2940 CE thermal analysis equipment from TA Instruments. AW7020 and AW6016 samples with plane parallel surfaces were placed vertically and held with a constant force of 0.05N. The temperature dependent change in length (Δl) was measured between 30°C and the solution heat treatment temperature at a heating rate of 10 K/min with a sensitivity of 0.1 μ m. Numerical derivative of smoothed curve of $\Delta l(T)/l(T)$ yields the instantaneous coefficient of linear thermal expansion CTE(T). The rate of expansion or contraction is compared with that of pure Al. DSC 2920 CE TA instrument was used for corresponding complementary tests with the same heating rate as applied in DIL. Pure aluminium was used as a reference sample for the DSC thermograms.

3. Results

3.1 Dilatometry and calorimetry curves after isothermal ageing of AW7020

The CTE curves of Fig. 1a) show that in the T4f condition the expansion accelerates up to 120°C (1) as compared with pure Al. There is no significant dilation difference to pure Al for 150°C/1h treatment up to 200°C as shown in Fig. 1a). There is a pronounced retardation of the expansion of the samples in T4f condition and in those aged at 150°C /1h around 260°C (3) and 250°C(3), respectively. The 150°C/24h aged sample shows an accelerated expansion up to 260°C (4) which continues further till 320°C (5) with a slight discontinuity in between at 290°C. All samples accelerate their expansion around 320°C (5). Fig. 1b) compares the DSC-thermograms of T4f with aged samples. An small endothermic peak up to about 200°C (1) is shown for the T4f. T4f and 150°C/1h conditions exhibit exothermic peaks at 250°C (3), where the 24h aged sample already behaves endothermic (4). All samples show a dominant endothermic effect from 300°C to 370°C (5).

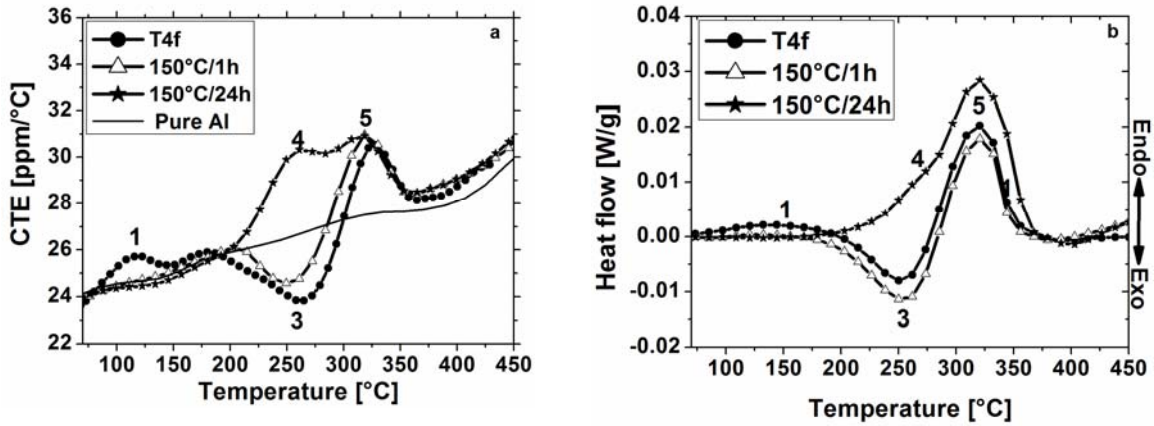


Fig. 1 AW7020 alloy in quenched (T4f) and isothermally heat treated conditions at 150°C for 1 and 24h: (a). CTE (T) compared with pure Al and (b) DSC thermograms.

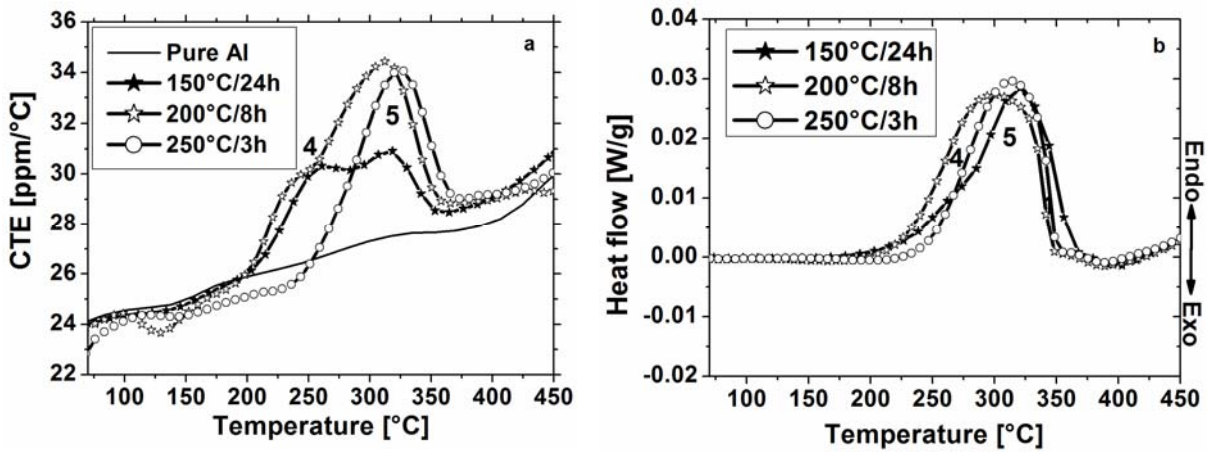


Fig. 2 AW7020 alloy in isothermally heat treated conditions at 150°C/24h, 200°C/8h and 250°C/3h: (a). CTE (T) compared with pure Al and (b) DSC thermograms.

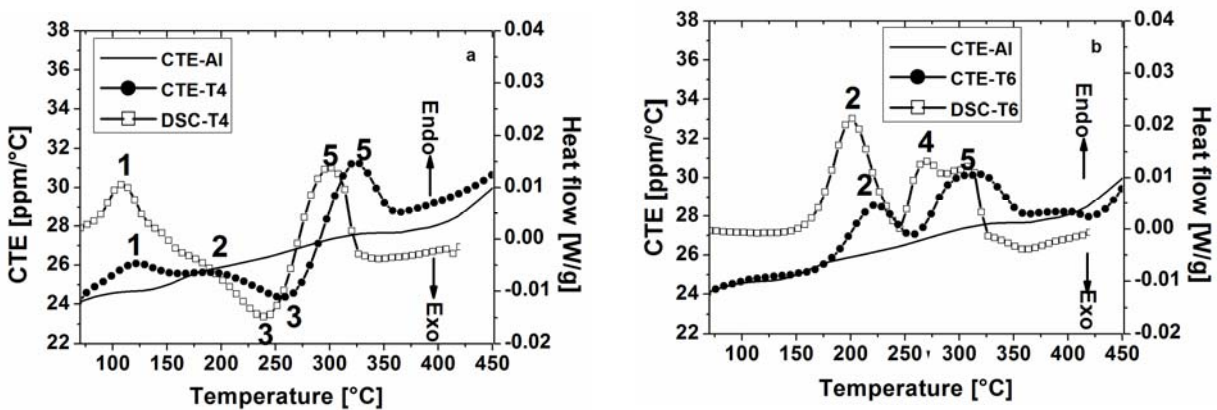


Fig. 3 CTE curves and DSC Thermograms of AW7020 alloy in (a) T4 condition; (b) T6 condition, compared with pure Al.

Accelerated expansion (5) is dominating at 200°C and 250°C in Fig. 2a). Only the 250°C/3h aged sample exhibits retardation up to 250°C which is within the scatter of the measurement. The CTE curve of the 200°C/8h aged sample shows a double peak (4)+(5). Thermograms in Fig. 2b) are dominated by endothermic peak (5), which starts faster for the 200°C/8h sample than for the others. In Fig.3a) and 3b), the CTE curves of T4 and T6 conditions are dominated by accelerated expansions at 120°C (1) and 215°C (2), respectively. A retardation peak (3) in the CTE curve

coincides with an exothermic peak at around 250°C of the T4 condition. Expansion is further dominating above 270°C (5). The T6 sample exhibits a double peak (4)+(5) in the thermogram. The CTE curves for T4 and T6 conditions were found to be late by about 20K with respect to the thermograms.

3.2 Precipitation kinetics of Si in Al-Mg-Si alloys

There is no significant dilatation difference between pure Al and AW6061 T4f. The CTE of AW6016 T4f shows an accelerated expansion between 300 and 410°C (peak at 374°C) with respect to pure Al followed by retardation. AW6016 T4fa and T4fb show similar expansion as T4f condition starting somewhat earlier at 240°C passing a maximum at 360°C, which is significantly smaller for T4fb. An AlSi1.7 alloy was used for comparison showing an accelerated expansion peak at 245°C as shown in Fig.4a). Fig.4b) exhibits accelerated expansion of AW6016 T4 from 210°C upwards accelerating above 270°C until 370°C with a peak at 310°C (i). AW6016 T4a shows an accelerated expansion from 270 to 350°C with a peak at 325°C (ii) followed by a significant retardation (v). T4b does not show any accelerated expansion but a continuous retardation above 350°C (v). AW6016 T4s and AlSi1.7 T4s accelerate their expansion from 230°C onwards slightly passing a maximum at 365 (iii) and 400°C (iv), respectively.

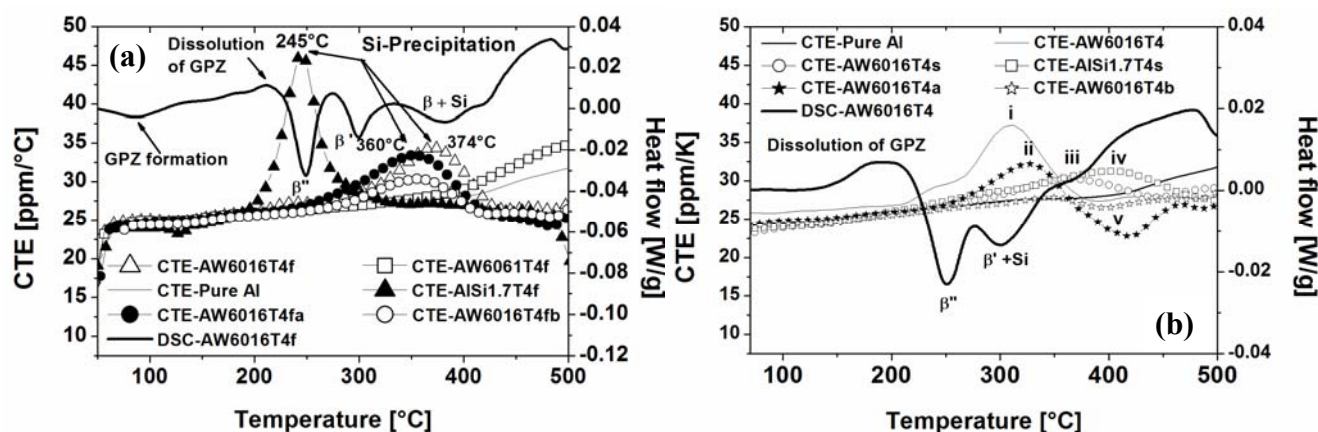


Fig. 4 (a) CTE curves and DSC thermograms of AW6016, AW6061, pure aluminium and AlSi1.7 [15] in T4f condition; (b) CTE curves of AW6016 in T4 condition, compared with pure Al and AlSi1.7.

4. Discussions

The results of AW7020 can be summarized in Table 1. Thus, peaks in CTE and DSC represent: (1) expansion and endothermic peaks at 120-200°C due to dissolution of GPI; (3) retardation in expansion and exothermic peak at around 250°C occurred due to precipitation of η'/η phase; (4) and (5) acceleration in the expansion and the endothermic peak at 265°C and 320°C, respectively, due to dissolution of η' and η . In the T4f condition the GPI precipitate during the thermal measurement (not detected), while in T4 condition the GPI are formed during the natural ageing and then dissolved during the thermal test. The aged conditions are characterized by the presence of η' and η in different amounts. The thermograph for 150°C/24h shows a shoulder (4) which is clearly separated in the CTE (T) curve related to the η' dissolution. GPI were found in T4 condition, while a coherent R-phase [18] is the main precipitate in T6 and is represented by peak (2). These phases dissolve during heating producing expansion (5) in Fig.3.

In the 6xxx alloys the Mg_2Si precipitates did not change the average atomic volume significantly. All the dilation differences with respect to pure Al are assigned to precipitation of free Si in Fig.4a). Mg/Si atom ratio is 1 in case of GPZ and β'' while it changes to 2 for β' and $\beta\text{-Mg}_2\text{Si}$ precipitates. In AlSi1.7 T4f, vacancy loops are available and easy precipitation of Si occurs around

245°C [15]. In AW6016 T4f condition, Si atoms are needed for GPZ formation. There, Si precipitation takes place only at 374°C, while in AW6016 T4 already at 310°C. Si precipitation occurs after dissolution of GPZ and β'' simultaneously with β' in T4 and with β in T4f as shown in Fig. 4a) and Fig. 4b). Dissolution of β'' and formation of β' and β releases Si, which can precipitate thereafter. During slowly cooling some Si precipitates, therefore the amount of Si precipitation is less in the T4s condition than in T4f condition, and a small Si-precipitation peak is observed in Fig.4b). In AW6061, the larger values in the CTE compared to that of pure Al above 380°C is related to Mg going into solution producing an expansion in the CTE curve.

Table 1 Correlation of DSC and DIL results with the phase transformation in AW7020
Abbreviations: Expansion: exp, Retardation: retard, Endothermic: endo, Exothermic: exo, p: peak position

Phases after heat treatment:	Dissolution of GPI (1) and R(2)	Formation of η' / η (3)	Dissolution of η' (4)	Dissolution of η (5)
T4: GPI	DIL: <150°C (exp) DSC: p:125°C (endo)	DIL: 220-290°C (retard) DSC: p:240°C (exo)		DIL: p:320°C (exp) DSC:p:340°C (endo)
T6: R + η' ,	DIL: 170-260°C (exp) DSC:p:200°C (endo)		DIL: >260-°C (exp) DSC: 250-280°C (endo)	DIL: p:330°C (exp) DSC: 280-320°C (endo)
T4f: GPI	DIL: <150°C (exp) DSC: <180°C (endo)	DIL: 200-300°C (retard) DSC: p:250°C (exo)		DIL: p:325°C (exp) DSC: p:325°C (endo)
150°C/1h: GPZ		DIL: p:250°C (retard) DSC: p:250°C (exo)		DIL: p:320°C (exp) DSC: p:320°C (endo)
150°C/24h: η' + η ,			DIL: p:260°C (exp) DSC: >225°C (endo)	DIL: p:320°C (exp) DSC:p:320°C (endo)
200°C/8h: η' ,			DIL: p:260°C (exp) DSC: >225°C(endo)	DIL: p:315°C (exp) DSC: p:300°C(endo)
250°C/3h: η ,				DIL: p:325°C(exp) DSC: p:315°C(endo)

5. Conclusions

1. Precipitation and dissolution in AW7020 alloy during continuous heating produces retardation and acceleration in the CTE (T), respectively.
2. Dilatometer and DSC measurements represent the precipitation kinetics in AW7020 correspondingly, except the dissolution of η differentiating two temperature ranges (4) and (5), which may be associated to different size classes.
3. Si precipitation in AW6016 with excess Si is shown as acceleration in the expansion during heating which appears at significant higher temperatures than in the Mg-free alloy: in the as quenched and in the slowly cooled condition around 370°C coinciding with β formation, in T4 around 310°C coinciding with β' formation. The second DIL/DSC cycles after interrupted heating treatments (T4fa,b, T4a,b) verify that Si precipitates once GPI and β'' are dissolved.
4. Precipitation and dissolution of Mg_2Si phase do not affect the CTE-curve. Mg_2Si and Si precipitation overlap in DSC thermograms.
5. Si precipitates simultaneously with β' in AW6016 T4 and with β - Mg_2Si in T4f conditions, respectively, and appear as superposed peaks during continuous heating in DSC. This superimposition can be separated and explained by DIL.

6. References

- [1] Takeo Sakurai, Kobelco Technology Review No. 28 (2008) 22-28.
- [2] Mun-Yong Lee, Sung-Man Sohn, Chang-Yong Kang, Dong-Woo Suh, Sang-Yong Lee, J. Mater. Process. Technol., 155-156 (2004) 1337-1343.
- [3] V. Hansen, O.B. Karlsen, Y. Langrudsrud and J. Gonnes, Mater. Sci. Technol. 20 (2004)
- [4] A. Zahra, C.Zahara, M.Laffite, W.Lacom, H.P.Degischer, Z.Metallkd,70 (1979) 172-179.
- [5] H.P.Degischer, W.Lacom, A. Zahra, C.Zahara, Z.Metallkd., 71 (1980) 231-238.
- [6] W.Lacom, H.P.Degischer , A. Zahra, C.Zahara, Z.Metallkd.,73 (1982)781-785.
- [7] K. Matsuda, S. Ikeno, H.Matsui, T. Sato, K. Terayama and Y. Uetani, Metall. Mater. Trans. A, 36A (2005) 2007-2012.
- [8] K. Matsuda, Y.Sakaguchi, Y. Miyata, Y. Uetani, T. Sato, A. Kamio, and S. Ikeno, J. Mat. Sci., 35 (2000) 179-189.
- [9] S. Müller, L. W. Wang, Alex Zunger, Phys. Rev. B: Condens. Matter, 60 (1999) 16448-16462.
- [10] C.Ravi, C. Wolvorton, Acta Mater.,52 (2004) 4213-4227.
- [11] C. Wolvorton, Acta Mater., 49 (2001) 3129-3142.
- [12] J. Major, E. Nagy, G. Tichy, Acta Phys, 40 (1976) 105-109.
- [13] F.Lasagni, A. Falahati, H. Mohamadian Semnani, H.P. Degischer, Kovove Mater., 46 (2008) 1-6
- [14] B. Verga, E. Fazakas, H. Hargitai, L.K. Verga, J. Phy: Conf.series, 144 (2009) 012105.
- [15] F. Lasagni, B. Mingler, M. Dumont, H.P. Degischer, Mat.Sci.Eng.A, 480 (2008) 383-391
- [16] A. Hayoune, D. Hamana, J. Alloys Compd. 474(2009) 118-123
- [17] L. Hadjadj, R. Amira, D. Hamana, A. Mosbash, J. Alloys Compd., 462(2008) 279-283.
- [18] W.Lacom, H.P.Degischer, A. Zahra, C.Zahara, Scripta Metall. 14 (1980) 253-254